THE ASTROPHYSICAL JOURNAL, 370:495–504, 1991 April 1

EXTRAGALACTIC GLOBULAR CLUSTERS. II. THE M31 GLOBULAR CLUSTER SYSTEM[1]

JOHN P. HUCHRA,[2] JEAN P. BRODIE,[3] AND STEPHEN M. KENT[2,4]
Received 1990 June 12; accepted 1990 September 14

ABSTRACT

We derive metallicities for 150 globular clusters associated with M31, using the strengths of six absorption features in the cluster integrated spectra. The properties of the M31 cluster system are very similar to those of the Milky Way system. We find no dependence of metallicity on cluster luminosity. The number distribution as a function of metallicity is consistent with that of Milky Way clusters. There is evidence for a weak metallicity gradient as a function of projected radius. The mean metallicity [Fe/H] is equal to -1.2, slightly higher than the mean for the Milky Way system. The distinction between the rotation of the metal-rich and metal-poor clusters is most apparent in the inner 2 kpc. Inside that radius the high-metallicity M31 clusters appear to form a central rotating disk. At large radii, the cluster system appears to be rotating with a semiamplitude of 60 ± 14 km s^{-1}; outside 10′ there appears to be no distinction in the rotation of the metal-poor and metal-rich clusters.

Subject headings: clusters: globular — galaxies: abundances — galaxies: individual (M31) — galaxies: internal motions — galaxies: stellar content

1. INTRODUCTION

A key question in understanding the formation of galaxies is the extent to which globular cluster properties depend on characteristics of the parent galaxy. This question has been difficult to address observationally because extragalactic clusters are usually faint and are superposed on background light from their parent galaxy. In most cases there are also problems in distinguishing bona fide clusters from foreground stars and background galaxies.

Because of its proximity, the obvious target for detailed study is the cluster system associated with our neighboring spiral galaxy, M31. Andromeda's was the first extragalactic globular cluster system to be discovered (Hubble 1932). Hubble was able to distinguish Andromeda's clusters on plates taken with the 100 inch (2.54 m) reflector at Mount Wilson because these clusters are spatially resolved. Since Hubble's identification of 140 cluster candidates, many authors have added to the list of cluster candidates (e.g., Seyfert & Nassau 1945; Mayall & Eggen 1953; Kron & Mayall 1960; Vetesnik 1962). The study of the Andromeda cluster system reawoke in the late 1970s, and the list of candidate clusters for Andromeda now totals over 500 (Sargent et al. 1977; Battistini et al. 1980; Buonano et al. 1982; Crampton et al. 1985; Battistini et al. 1987).

The first detailed spectroscopic and photometric study of the cluster system was done by van den Bergh (1969) with the Palomar 200 inch (5.08 m) Hale Telescope. Van den Bergh measured a line-strength index in his low-resolution (50 Å mm^{-1}) spectra, and found that the M31 clusters appeared to be, on average, more metal-rich than Galactic globulars. The metallicity of the clusters did not appear to be a function of radius, but most of his clusters were inside 50′. Van den Bergh also measured velocities for 33 clusters. Spinrad & Schweizer (1972) observed eight M31 clusters and found a range of metallicities similar to that seen by van den Bergh. They also suggested that three of the clusters were "super–metal-rich."

Huchra, Stauffer, & van Speybroeck (1982, hereafter HSS), obtained spectra of ~60 M31 clusters with the MMT and found that the cluster system exhibits significant rotation (~80 km s^{-1}), comparable to the ~60 km s^{-1} rotation velocity for the Galactic globular cluster system (Frenk & White 1980). The discovery of rotation has important implications for the formation and evolution of globular cluster systems, since it requires either that the clusters were formed from a slowly rotating system or that the cluster (or some of them) have been tidally spun up by interactions with the disk. The latter possibility is more likely given the nearly spherical shape of the halo.

Since the discovery of the rotation of the Andromeda and Milky Way cluster systems, a small controversy has arisen over whether or not these systems can be broken into distinct kinematic subsamples. Although the situation for the Galaxy was initially somewhat muddled (Frenk & White 1982), most recent analyses have tended to confirm the dual nature of the cluster kinematical population (Zinn 1985, 1986). Essentially, the metal-poor clusters ([Fe/H] ≤ -0.8) in the Galaxy form a slowly rotating ($V_r \sim 60$ km s^{-1}), spheroidal population, while the metal-rich systems are more disklike as well as much more rapidly rotating ($V_r \sim 150$ km s^{-1}).

A similar result has been quoted by Freeman (1983, 1985) and Searle (1983) for the Andromeda system based on HSS velocities and spectral for 61 clusters. Dividing the M31 clusters at [Fe/H] $= -0.6$, Freeman found that the metal-poor clusters are not rotating at all and have a velocity dispersion of only 90 km s^{-1}. He claimed that the metal-rich clusters essentially follow the disk Population I rotation curve. Later, Searle, using his own unpublished sample of 100 clusters, no longer saw any evidence of a separate disk population of M31 globular clusters (Searle 1986, quoted in Zinn 1986). Assigning metallicity to M31 clusters on the basis of color, Elson & Walterbos (1988) constructed three metallicity groups and found that the metal-rich clusters formed a disk, while the metal-poor clusters showed little evidence for rotation and

[1] Work reported here based on observations made with the Multiple Mirror Telescope, a joint facility of the Smithsonian Institution and the University of Arizona.

[2] Harvard-Smithsonian Center for Astrophysics, 60 Garden Street, Cambridge, MA 02138.

[3] Lick Observatory, University of California, Santa Cruz, CA 95064.

[4] Presidential Young Investigator.

were significantly more extended than the intermediate-metallicity group.

Spectra of an additional ~90 M31 clusters have since been obtained at the MMT. These new observations provide velocities for all clusters brighter than $V \sim 16.5$ (based on the magnitudes given by Battistini et al. 1980), as well as many fainter clusters at large projected radii. Velocities for the complete sample of 149 clusters were used by Kent, Huchra, & Stauffer (1989) to examine the mass distribution in M31. Although no strong constraints could be placed on the relative contributions of halo and disk, the mass distribution was found to be consistent with that inferred from M31's rotation curve. The velocity dispersion was revised upward from 128 km s^{-1} found by HSS to ~155 km s^{-1}, presumably because of the larger sample. The rotation of the cluster system was revised downward to $\sim 45 \pm 13$ km s^{-1}, and the mean velocity changed from -281 to -270 ± 25 km s^{-1}. The velocity of M31 itself is -297 km s^{-1} (Rubin & Ford 1970).

Below we derive metallicities for the 150 M31 clusters using a new method for the determination of metallicities of composite systems (Brodie & Huchra 1990). We then use these estimates with the velocity information to explore the metallicity/kinematic properties of the M31 cluster system and discuss similarities and differences with the Milky Way system.

2. THE DATA

The observational details are identical to those given in Kent, Huchra, & Stauffer (1989) and Brodie & Huchra (1990). The majority of the data have been taken with an S20 magnetically focused EMI image tube (Cromwell & Weymann 1982) with a fibre-optic reducing boule between the image tube and the Reticon (Latham 1982). This system has a spectral resolution of ~8 Å and enhanced blue sensitivity. These observations extend to the atmospheric cutoff at 3200 Å.

2.1. *Radial Velocities*

Radial velocities were obtained using standard cross-correlation techniques (Tonry & Davis 1979) and templates made from high signal-to-noise spectra of M31, M32, NGC 4486B (a compact dwarf near M87), and two M31 globular clusters, 163-217 and 225-280. The original HSS observations cover the wavelength range 3800–6500 Å at a resolution of 5–6 Å. Velocities were obtained from these data with rms accuracies of about 30 km s^{-1}. The newer observations have slightly lower resolution, ~8 Å, but extend to the atmospheric cutoff, so that while they provide much better wavelength coverage and thus metallicity measurements, the velocities from single measurements are degraded to about 45 km s^{-1} rms. Many of the objects that were observed by HSS were reobserved in order to provide a sample with homogeneous wavelength coverage. A few additions have been made to the compilation given in Kent, Huchra, & Stauffer (1989).

We have checked our velocities against those from several sources, including those of Federici, Fusi Pecci, & Marano (1990) and the high-precision echelle velocities of Peterson (1990). For the 14 clusters we have in common with Peterson, there is a mean offset of $V_{HBK} - V_P = 16$ km s^{-1} and a dispersion of 26 km s^{-1}, which is fully consistent with the expected dispersion of 24 km s^{-1} calculated from the quadrature of our estimated errors and Peterson's. For the three high signal-to-noise template quality objects, 225-280, 158-213, and 163-217, our average offset is less than 3 km s^{-1}. For the 19 clusters we have in common with Federici et al., there is a mean offset of $V_{HBK} - V_F = -13$ km s^{-1}, and a dispersion of 60 km s^{-1}, which is consistent with their estimated error of ~50 km s^{-1}. The mean velocity of the 150 clusters currently in our sample is -267 ± 13 km s^{-1}, approximately 2 σ lower than M31's 21 cm velocity of -297 km s^{-1}. The mean velocity given here is slightly lower that that quoted by Kent, Huchra, & Stauffer (1989) because of additional data.

2.2. *Abundances*

As part of a study of various late-type stellar populations, including globular cluster systems and elliptical, dwarf, and S0 galaxies, we have devised a robust method of metallicity determination. The method, described in detail in Brodie & Huchra (1990), uses six absorption-line indices measured from integrated cluster spectra to provide metallicity, [Fe/H], estimates which are, in principle, good to ~15%. The method is designed to be as impervious as possible to observational errors and abundance anomalies. The features found to provide the best estimates of [Fe/H] measure the strengths of the Fraunhofer line blanketing discontinuity at 4000 Å, the blue cyanogen feature at 3883 Å, the CH G band, magnesium hydride, the magnesium *b* triplet, and Fe λ5270. The calibrations are based on observations of well-studied Galactic and M31 clusters and are tied to the metallicity scale of Zinn & West (1984). A weighted mean of the six estimates is used to determine the final [Fe/H] value for each cluster.

2.3. *Geometry*

We have derived the relative coordinates of the globular clusters assuming standard geometric parameters for M31. We take the galaxy's center as

$$\alpha = 00^h40^m00^s.1 , \quad \delta = +40°59'43'' \quad (1950) , \qquad (1)$$

and the position angle of the major axis as 38° (Baade & Arp 1964; Kent 1989). The X and Y coordinates of the clusters (where X is the coordinate parallel to the major axis) are given by the equations

$$x' = \sin(\alpha - \alpha_0)\cos\delta , \qquad (2)$$

$$y' = -\cos(\alpha - \alpha_0)\cos\delta\sin\delta_0 + \sin\delta\cos\delta_0 , \qquad (3)$$

$$X = x'\sin\theta + y'\cos\theta \qquad (4)$$

$$Y = -x'\cos\theta + y'\sin\theta \qquad (5)$$

where α_0 and δ_0 are the coordinates of the center of M31, and $\theta = 38°$ is the major-axis position angle. The projected radius, R, is the quadrature sum of X and Y. In this coordinate system, positive X is east by northeast and positive Y is north by northwest.

Metallicities and velocities and their associated errors for the 150 M31 clusters are given in Table 1 along with coordinates and the projected radius, R, and distance from the minor axis, X. The cluster "names" are the combination of the designations given by the Italian group (Battistini et al. 1980 and following papers) and by Sargent et al. (1977). For example, "291-9" is object 219 in the Battistini et al. (1980) list and object 9 in the Sargent et al. (1977) list. Additional designations are given in the notes. The V-magnitudes for the clusters are from Battistini et al. (1980) where available; otherwise they are from Battistini et al. (1987) and van den Bergh (1969). Since the original sample of cluster candidates was selected for observation (to a magnitude limit of ~16.5) based on the 1980 paper, we prefer to quote those here even though the magnitudes in

TABLE 1

M31 GLOBULAR CLUSTERS

Name (1)	α (1950) (2)	δ (3)	V (4)	v_h (5)	R (6)	X (7)	[Fe/H] (8)	Notes (9)
000-001	00:30:05.6	39:18:09	13.70	-331± 24	152.3	-149.5	-1.08± 0.09	M II (332.1±3 rp)
000-2	00:30:52.5	39:14:48	15.80	-380± 51	148.2	-146.8	-1.70± 0.36	M III
293-11	00:33:38.0	40:37:07	16.39	-345± 35	75.7	-61.9	-1.89± 0.17	L
295-14	00:34:04.0	40:03:12	16.63	-320± 43	88.2	-86.0	-1.91± 0.36	S2,BA19
298-21	00:35:17.4	40:27:27	16.53	-438± 62	62.5	-58.2	-2.19± 0.56	
000-25	00:35:59.5	41:27:32		79± 65	53.1	-5.6	-1.80± 0.65	N205?
000-27	00:36:11.9	40:18:29		-165± 49	59.8	-59.1	-1.23± 0.57	V6 (too near bright star?)
306-29	00:36:25.7	40:17:52		-421± 37	58.4	-58.0	-0.64± 0.40	V2,BA18
311-33	00:36:50.7	40:14:46	15.50	-507± 43	57.5	-57.5	-1.74± 0.17	V4,BA17
312-35	00:36:57.0	40:40:35	15.53	-218± 31	39.6	-36.3	-1.71± 0.40	V19
315-38	00:37:05.4	40:15:03	16.28	-291±108	55.6	-55.6	-1.88± 0.52	V5,BA14, poor vel
001-39	00:37:08.0	40:41:44	16.80	-213± 39	37.2	-34.1	-0.29± 0.72	
317-41	00:37:11.8	41:31:19	16.61	-7± 74	44.7	5.6	-2.12± 0.36	N205-H VIII
318-42	00:37:17.7	40:17:41	16.97	-384± 82	52.1	-52.1	-2.10± 0.50	V7
004-000	00:37:34.7	41:06:14	16.60	-277± 53	28.2	-11.7	-1.26± 0.59	
005-52	00:37:37.2	40:27:03	15.80	-235± 13	42.4	-42.4	-0.68± 0.34	V16
328-54	00:37:41.1	41:23:56	18.52	-348	35.6	3.1	-1.22± 0.80	N205-H IV, V233
000-55	00:37:41.3	41:26:27		-67± 44	37.4	5.1	-1.07± 0.55	N205
006-58	00:37:43.1	41:11:00	15.80	-213± 22	28.2	-6.9	-0.57± 0.15	V55
009-61	00:37:47.4	41:20:30	16.90	-335± 52	32.5	1.1	-1.57± 0.26	HI
010-62	00:37:48.2	40:57:56	16.70	-77± 66	25.0	-16.7	-1.87± 0.61	V37
011-63	00:37:48.6	41:22:52	16.60	-157± 52	33.9	3.1	-1.54± 0.34	N205?
012-64	00:37:49.1	41:05:17	15.00	-373± 33	25.3	-10.7	-1.81± 0.30	V301
017-70	00:38:05.2	40:55:04	15.70	-497± 27	22.2	-17.0	-1.23± 0.52	V38
019-72	00:38:09.1	41:02:03	14.60	-205± 16	21.1	-11.0	-1.14± 0.16	V44 (-224.0±2.5 rp)
020-73	00:38:11.7	41:25:00	14.60	-348± 11	32.5	7.5	-1.07± 0.10	N205-H III (-349.0±2.1 rp)
338-76	00:38:15.5	40:19:21	14.39	-238± 15	45.0	-44.0	-1.34± 0.08	V12 (-275.6±2.9 rp)
023-78	00:38:17.5	40:57:02	14.20	-414± 14	19.6	-14.0	-0.92± 0.10	V42 (-454.4±5.5 rp)
024-82	00:38:28.1	41:29:25	16.80	-289± 34	34.4	12.8	-0.48± 0.30	V268
027-87	00:38:30.9	40:39:02	15.60	-266± 37	26.7	-26.7	-1.64± 0.32	V27
029-90	00:38:34.1	40:43:56	16.70	-412± 41	22.7	-22.4	-0.44± 0.15	V29 (-374.0±2.7 rp)
034-96	00:38:44.4	40:37:02	15.40	-546± 28	26.8	-26.7	0.31± 2.08	V26
038-98	00:38:52.1	41:02:48	16.50	-111± 58	13.2	-5.4	-1.74± 0.68	V59
039-101	00:38:54.0	41:04:02	15.80	-197± 31	13.2	-4.3	-0.95± 0.56	V65
042-104	00:38:57.8	40:50:06	15.90	-309± 31	15.2	-14.8	-1.09± 0.84	V227
343-105	00:38:58.6	39:55:56	16.35	-442± 38	64.8	-57.5	-1.49± 0.17	V199
043-106	00:38:58.7	40:26:14	16.50	-440± 65	35.4	-33.6	-2.13± 0.61	V21, poor vel
044-107	00:38:58.9	41:03:39	16.50	-279± 49	12.2	-4.0	-1.14± 0.37	
045-108	00:38:59.2	41:17:05	15.80	-383± 30	20.8	6.7	-0.94± 0.27	V94
046-109	00:39:00.8	41:30:03	17.50	-77± 49	32.3	17.1	-1.84± 0.61	V280
047-111	00:39:01.6	41:25:39	17.30	-126± 58	28.2	13.7	-1.61± 1.20	V103
048-110	00:39:01.6	40:57:04	16.50	-163± 49	11.4	-8.9	-0.59± 0.74	S10
051-114	00:39:02.7	41:08:05	16.00	-259± 31	13.7	0.0	-0.80± 0.31	V79
058-119	00:39:09.2	40:30:04	15.00	-210± 16	31.2	-29.3	-1.45± 0.24	V23 (-223.5±4.4 rp)
061-122	00:39:16.1	41:13:09	16.50	-246± 47	15.8	5.5	-0.79± 0.33	V259
063-124	00:39:16.7	41:12:04	15.80	-281± 34	14.8	4.7	-0.87± 0.33	V258
064-125	00:39:18.0	40:54:04	16.00	-286± 45	9.8	-9.3	-1.55± 0.30	V49
065-126	00:39:18.0	40:23:45	16.70	-416± 47	36.8	-33.3	-1.01± 0.29	V200
344-127	00:39:19.0	41:35:37	15.78	-252± 21	36.7	23.6	-1.13± 0.22	V295
068-130	00:39:19.3	40:42:23	16.30	-257± 33	19.0	-18.4	-0.29± 0.59	V32
073-134	00:39:23.4	40:42:06	16.00	-463± 26	18.9	-18.2	-0.64± 0.46	V33
074-135	00:39:23.9	41:26:57	16.50	-405± 61	28.1	17.3	-1.80± 0.66	V105
076-138	00:39:26.2	40:48:06	17.10	-587± 46	13.3	-13.1	-1.35± 0.63	V43
082-144	00:39:31.8	40:44:05	15.60	-325± 18	16.5	-15.6	-0.86± 0.61	V39 (-364.3±3.2 rp)
083-146	00:39:32.2	41:28:56	16.80	-209± 41	29.7	19.8	-1.27± 0.35	V107

TABLE 1—*Continued*

Name (1)	α (2)	δ (3)	V (4)	v_h (5)	R (6)	X (7)	[Fe/H] (8)	Notes (9)
085-147	00:39:34.5	40:23:31	16.70	-505± 68	36.5	-31.5	-1.83± 0.40	V201
086-148	00:39:34.6	40:57:04	14.80	-168± 21	5.5	-5.1	-1.74± 0.17	V62
088-150	00:39:36.9	41:15:05	15.40	-378± 45	16.0	9.4	-2.17± 0.48	V97
092-152	00:39:38.3	40:51:04	16.90	-410± 38	9.6	-9.4	-1.65± 0.49	V239
093-155	00:39:39.0	41:05:17	16.70	-502± 46	6.8	1.9	-1.25± 0.19	V82
094-156	00:39:41.0	40:40:05	15.80	-558± 23	20.0	-17.7	-0.41± 0.31	V35
095-157	00:39:41.8	40:49:01	16.10	-162± 33	11.2	-10.6	-1.57± 0.41	V46
096-158	00:39:42.0	41:02:48	16.40	-310± 50	4.6	0.3	-0.26± 0.43	V87
098-000	00:39:43.4	40:43:10	16.40	-247± 30	16.8	-15.0	-0.67± 0.58	compact
102-000	00:39:45.6	41:17:52	16.50	-205± 50	18.4	12.6	-1.59± 0.31	compact
103-165	00:39:45.6	41:01:03	15.10	-323± 22	3.0	-0.6	-0.56± 0.62	V75
106-168	00:39:46.9	40:55:52	16.30	-90± 43	4.6	-4.6	-0.86± 0.68	V61
107-169	00:39:47.1	41:03:01	15.70	-311± 30	4.1	1.1	-1.18± 0.30	V80
109-170	00:39:48.1	40:54:02	16.40	-613± 24	6.1	-5.9	-0.31± 0.78	V56
110-172	00:39:49.1	40:47:00	15.60	-232± 27	12.9	-11.3	-1.00± 0.51	V231
112-174	00:39:49.1	41:01:16	16.30	-286± 34	2.6	-0.1	0.29± 0.49	V77
115-177	00:39:50.3	40:57:04	16.00	-497± 29	3.2	-3.2	-0.15± 0.38	V67
116-178	00:39:50.3	41:16:03	16.60	-305± 27	16.4	11.7	-0.76± 0.52	V269
117-176	00:39:50.3	40:40:43	16.40	-487± 58	19.1	-16.1	-1.75± 0.46	V36
121-000	00:39:54.5	41:03:55	16.50	-3± 33	4.3	2.7	0.14± 1.01	compact
352-180	00:39:53.8	41:45:48	16.37	-143± 50	46.1	35.6	-1.88± 0.83	
127-185	00:40:00.0	40:58:02	15.50	-483± 25	1.7	-1.3	-1.08± 0.24	V70
131-189	00:40:06.3	41:00:04	16.00	-424± 28	1.2	1.0	-0.81± 0.28	V81
135-192	00:40:07.7	41:14:04	16.10	-386± 32	14.4	12.2	-1.62± 0.20	V271
143-198	00:40:15.4	41:02:05	16.00	-107± 23	3.7	3.6	0.09± 0.42	V88
146-000	00:40:18.7	40:58:06	16.80	-228± 61	3.9	0.9	-0.43± 0.81	
147-199	00:40:19.1	41:04:06	15.50	-89± 12	5.7	5.7	-0.24± 0.36	V91 (-88.6±3.6 rp)
148-200	00:40:19.6	41:01:04	15.80	-315± 42	3.9	3.3	-1.53± 0.39	V86
000-202	00:40:21.9	41:45:23		-230± 80	45.8	38.5	-2.08± 0.70	
151-205	00:40:25.3	41:05:01	14.70	-297± 22	7.1	7.1	-0.75± 0.18	V93
152-207	00:40:25.8	41:01:50	16.20	-108± 34	5.3	4.7	-0.87± 0.49	V89
153-000	00:40:26.3	40:58:03	16.00	-187± 23	5.2	1.7	-0.08± 0.33	
154-208	00:40:28.2	40:59:39	16.72	-178± 33	5.3	3.2	-0.45± 0.63	V84
357-209	00:40:29.3	39:54:31	16.50	-277± 25	65.4	-47.9	-0.80± 0.42	metal rich
158-213	00:40:30.2	40:50:06	14.50	-180± 8	11.2	-4.1	-1.08± 0.05	V64 (-186.5±5.9 rp)
161-215	00:40:31.2	40:54:59	16.40	-398± 45	7.5	-0.1	-1.25± 0.35	V252
163-217	00:40:33.3	41:11:02	14.80	-162± 7	12.9	12.8	-0.36± 0.27	V100 (-161.0±3.8rp)
165-218	00:40:34.0	40:54:29	16.30	60± 54	8.3	-0.2	-1.80± 0.32	V74
166-000	00:40:36.2	40:56:08	16.50	-3± 37	7.7	1.4	-1.40± 0.54	compact
358-219	00:40:34.2	39:32:48	15.10	-270± 59	87.2	-64.4	-1.83± 0.22	M IV
171-222	00:40:41.3	40:59:01	15.00	-231± 17	7.8	4.2	-0.48± 0.26	V87 (-273.0±2.7rp)
174-226	00:40:45.8	41:22:03	15.40	-478± 31	23.9	22.9	-1.67± 0.27	V115
175-000	00:40:45.8	40:58:11	16.50	76± 25	8.8	4.1	-1.28± 0.61	
176-227	00:40:46.3	40:32:46	16.30	-499± 53	28.3	-15.8	-1.59± 0.64	V30
178-229	00:40:46.5	41:04:05	14.70	-119± 26	9.8	8.8	-1.51± 0.12	V95
179-230	00:40:46.8	41:01:05	15.20	-139± 25	8.9	6.5	-1.21± 0.33	V92 (-137.8±2.2 rp)
180-231	00:40:47.5	40:51:02	15.90	-155± 40	12.5	-1.3	-1.53± 0.41	V249
182-233	00:40:52.4	40:51:05	15.00	-300± 23	13.1	-0.7	-1.19± 0.23	V73 (-349.3±4.9 rp)
183-234	00:40:52.7	40:45:04	16.10	-207± 34	17.7	-5.4	-0.19± 0.31	V57
185-235	00:40:53.0	40:58:02	15.70	-151± 28	10.1	4.8	-1.03± 0.22	V90
193-244	00:41:00.9	41:20:03	15.30	-48± 23	23.3	23.1	-0.35± 0.25	V116 (-58.6±2.1 rp)
201-250	00:41:08.6	40:53:03	15.50	-734± 31	14.6	2.7	-1.06± 0.21	V83
204-254	00:41:12.0	41:05:04	15.80	-321± 26	14.6	12.6	-1.17± 0.37	V275
205-256	00:41:13.7	41:08:01	15.40	-352± 19	16.2	15.1	-1.34± 0.13	V102
206-257	00:41:14.1	41:13:05	15.20	-151± 23	19.3	19.1	-1.45± 0.10	V106
209-261	00:41:18.2	41:09:02	16.50	-390± 33	17.4	16.4	-1.38± 0.27	V284

TABLE 1—*Continued*

Name (1)	α (2)	δ (3)	V (4)	v_h (5)	R (6)	X (7)	[Fe/H] (8)	Notes (9)
211-262	00:41:18.6	41:03:40	16.40	-39± 47	15.3	12.2	-1.67± 0.52	V98
212-263	00:41:18.8	40:48:03	14.80	-326± 40	18.9	0.0	-1.75± 0.13	V76
213-264	00:41:19.0	41:14:01	16.80	-596± 38	20.6	20.4	-0.99± 0.39	V292
216-267	00:41:24.3	41:21:32	17.20	-96± 20	27.0	26.9	-2.04± 1.07	V119, young
217-269	00:41:26.0	41:07:26	16.20	58± 28	17.9	16.1	-0.59± 0.65	V281
218-272	00:41:29.9	41:02:06	14.70	-210± 12	17.1	12.3	-1.18± 0.22	V101 (-225.0±4.3 rp)
219-271	00:41:30.7	40:40:23	16.40	-526± 28	25.8	-4.6	-0.73± 0.53	V58
220-275	00:41:34.8	41:14:11	16.50	-300± 68	23.0	22.4	-2.07± 0.82	V114
221-276	00:41:38.4	41:16:43	16.60	-337± 41	25.1	24.8	-1.26± 0.50	V117
224-279	00:41:42.5	41:12:03	15.30	-103± 38	22.9	21.6	-1.90± 0.24	V112,BA1 (-161.2±2.2 rp)
225-280	00:41:45.1	41:05:12	14.30	-164± 3	20.5	16.4	-0.70± 0.12	V282 (-167.0±7.7 rp)
228-281	00:41:48.4	41:25:05	16.70	-475± 34	32.5	32.5	-0.65± 0.66	V131
229-282	00:41:49.0	41:22:05	16.90	-103± 88	30.3	30.2	-1.81± 0.74	V120,S15
230-283	00:41:50.8	40:40:05	16.00	-448± 45	28.7	-2.5	-1.94± 0.27	V303
232-286	00:41:55.8	40:58:04	15.50	-151± 23	21.9	12.2	-1.77± 0.24	V99
233-287	00:41:57.1	41:27:03	15.70	-89± 32	35.1	35.1	-1.59± 0.32	V121
366-291	00:42:01.9	41:47:27	16.31	-202± 52	52.9	51.6	-1.39± 0.28	V134,BA24
235-297	00:42:13.3	41:13:00	16.30	-106± 33	28.4	26.0	-1.32± 0.36	V299
370-300	00:42:29.5	41:41:17	16.14	-423± 52	50.1	50.0	-1.61± 0.29	V130,BA23
238-301	00:42:30.1	41:03:14	16.50	11± 34	28.5	20.3	-1.22± 0.76	V108
239-000	00:42:30.7	41:18:54	16.90	-390± 51	34.2	32.6	-1.18± 0.61	
240-302	00:42:40.4	40:49:06	14.90	-8± 32	32.1	10.4	-1.76± 0.18	V196
372-304	00:42:48.3	41:44:02	16.48	-242± 38	54.4	54.3	-1.28± 0.31	V136,BA26
373-305	00:42:56.9	41:29:11	15.63	-205± 18	44.4	43.7	-0.50± 0.22	V125,BA2
375-307	00:43:00.5	41:23:18	17.54	-196± 70	41.3	39.5	-1.23± 0.22	
377-308	00:43:03.5	40:21:42	17.03	-46± 52	51.5	-8.3	-2.19± 0.65	star??
376-309	00:43:03.5	41:26:17	18.12	-142± 20	43.5	42.2	-2.18± 0.99	V124 young
379-312	00:43:14.0	40:26:09	16.05	-352± 32	49.8	-3.6	-0.70± 0.35	
381-315	00:43:22.2	41:04:35	15.55	-103± 34	38.4	27.4	-1.22± 0.43	V118 (-85.8±1.9 rp)
486-316	00:43:23.5	40:41:41	17.58	-131± 45	42.5	9.7	-2.28± 0.98	
384-319	00:43:37.4	40:00:37	15.75	-353± 19	72.1	-20.8	-0.66± 0.22	V197
386-322	00:43:41.7	41:45:31	15.59	-349± 16	61.8	61.7	-1.21± 0.38	BA8
387-323	00:43:48.7	40:27:51	17.09	-276± 78	53.8	1.8	-1.96± 0.29	
000-327	00:44:03.6	42:28:26	16.00	-326± 31	99.7	97.7	-1.76± 0.11	M VI
397-336	00:44:42.1	40:55:49	16.32	-207± 50	53.4	30.0	-1.05± 0.53	V195
403-348	00:46:32.0	41:18:48	16.31	-337± 48	76.2	60.9	-0.45± 0.78	
405-351	00:46:47.1	41:19:12	15.18	-208± 37	79.0	63.0	-1.80± 0.31	V140
407-352	00:47:23.8	41:24:41	16.01	-326± 20	87.1	71.6	-0.85± 0.33	MV
000-355	00:48:48.1	39:41:16	15.40	-66± 49	127.5	1.7	-1.31± 0.67	

NOTE.—Alternative designations are from Hubble 1932 (denoted by H), Vetesnik 1962 (V), Baade & Arp 1964 (BA), and Mayall & Eggen 1953 (M). Notes to individual objects are given below.

000-25: Probably a cluster (Cohen 1987).
000-27: MMT coordinates 00:36:10.6 + 40:18:34.
000-54: Velocity from van den Bergh 1969; ours is −225 ± 98.
10-62: Extended image viewed at MMT.
47-111: Previously suspected open cluster, but our spectrum shows it to be a globular.
63-124: Very stellar, globular spectrum.
93-155: Peculiar spectrum.
110-172: Stellar.
112-174: Some contamination from bulge, possibly why [Fe/H] is so high.
115-177: Emission lines seen in the Reticon spectra of this object are due to galaxy contamination. Object observed with 1″ circular apertures.
147-199: Van den Bergh's 1969 ID or velocity for V91 are probably incorrect, since our velocity and Peterson's agree so well.
163-217: Object used as an MMT velocity template.
166-000: Slightly extended at MMT.
211-262: In OB36.
000-267: Extended at MMT.
225-280: Object used as an MMT velocity template.
000-308: Probably a cluster (Cohen 1987).
000-309: Extended at MMT.
387-323: Diffuse; MMT coordinates 00:43:47.8 + 40:27:54.
405-351: MMT coordinates 00:46:53.6 + 41:19:11 for object 351 on chart of Sargent et al. 1977.
000-355: Extended at MMT.

TABLE 2

OTHER OBJECTS

Name (1)	α (1950) (2)	δ (3)	V (4)	V_h (5)	Notes (6)
Background Galaxies					
000-3	00:31:06.0	41:47:16		34389±107	plus superposed K star
000-4	00:31:57.7	39:18:08		5804± 77	
000-5	00:32:19.6	42:12:40		24656± 54	
000-6	00:32:22.3	42:19:02		19761± 45	
000-7	00:32:31.1	42:18:49		24669± 29	
000-8	00:33:10.5	39:40:38		30181± 58	BA20
296-15	00:34:04.4	40:14:17	17.64	30079± 32	
297-16	00:34:10.0	39:22:09	17.53	5721±120	BA16
000-145	00:39:32.3	40:03:11		30764± 41	Seyfert 1
000-225	00:40:45.4	38:55:16		25318± 81	S13, Seyfert 2
000-273	00:41:32.2	42:40:39		35118± 37	very blue
000-294	00:42:03.4	42:43:59		14076± 34	
394-331	00:44:20.3	40:51:50	17.23	15546± 48	
000-345	00:45:38.3	40:13:00	18.67	39893± 51	
000-347	00:46:13.0	42:25:17		10250± 38	BA12, emission
000-349	00:46:43.2	39:46:28		23502± 35	
408-354	00:47:44.0	40:19:11	16.87	40322± 45	
Confirmed Stars, etc.					
000-13	00:33:55.8	41:59:58	18.3	47± 38	
000-17	00:34:30.2	39:33:37		-90± 38	K-M star
GS-1	00:40:03.5	40:59:13		-1± 41	
000-320	00:43:39.4	40:13:48		-7± 34	
000-324	00:43:48.8	41:55:20		-44± 36	HII Region
GS-SET	01:13:05.4	49:20:42	15.99	-187± 45	a.k.a. vdB (-32+/-20 bff)

NOTES.—000-3: K star, $v \sim 17$, to southeast of galaxy. GS-SET is the distant globular cluster suspect from Sargent et al. 1977, and has also been observed by Bónoli, Federici, & Fusi Pecci 1988 (= bff).

the 1987 paper are more precise. The precise echelle velocities from Peterson (1990) are given in the notes and marked "rp." The line indices for the M31 clusters, as well as a large sample of other globular clusters and galaxies, are given in Huchra et al. (1991).

In addition to the spectroscopically confirmed globular clusters, an additional 23 candidate objects were observed that are either background galaxies, foreground Galactic stars, or compact H II regions (e.g., Huchra & Brodie 1984). These objects are listed in Table 2.

3. KINEMATICS AND METALLICITY

3.1. *Mass Estimate*

Figure 1 shows the cluster radial velocities as a function of distance along the major axis of the galaxy. The slight rotation of the cluster system is apparent. A simple dynamical analysis can be done using either the virial or projected mass estimators (Bahcall & Tremaine 1981; Heisler, Tremaine, & Bachall 1985; see Huchra & Brodie 1987 or van den Bergh 1981 for examples). We assume that the distance of M31 is 690 kpc. The measured line-of-sight velocity dispersion, σ_V, is equal to 155 km s^{-1}. Both estimators give the galaxy' mass (and thus mass-to-light ratio) as

$$M \sim 3.1 \pm 0.5 \times 10^{11}\ M_\odot\ , \quad (6)$$

and on the fully corrected B_T system,

$$M/L_{B_T^c} \sim 16 \pm 3\ M_\odot/L_\odot\ , \quad (7)$$

or the $B(0)$-Zwicky system (Huchra 1976),

$$M/L_B(0) \sim 40 \pm 7\ M_\odot/L_\odot\ , \quad (8)$$

in very good agreement with the 21 cm rotation curve mass for M31 (Roberts & Whitehurst 1975) and the values of M/L determined for other rotating spiral galaxies (Faber & Gallagher 1979).

3.2. [Fe/H] *versus Radius*

The distribution of metallicities in the galaxy halo provides a fundamental test of chemical enrichment in collapsing protogalaxies. Figure 2 shows the M31 cluster metallicity as a function of projected radius. Only those (96) objects for which the error in the metallicity estimate is 0.5 dex or less are plotted. There is a measurable, but weak, metallicity gradient; in particular, the scatter in [Fe/H] is large at small projected radii

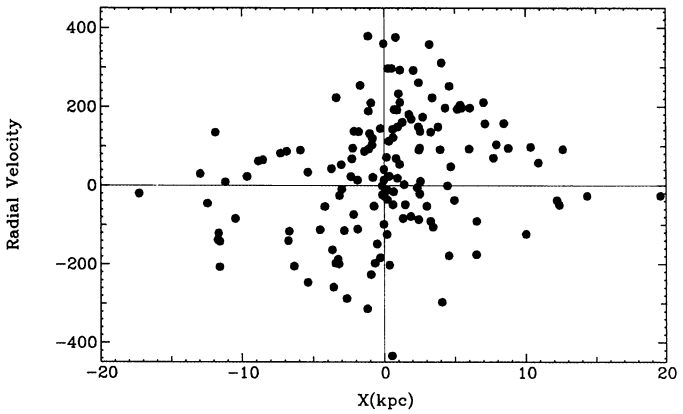

FIG. 1.—Velocity vs. x, the projected distance from the minor axis, in kpc. The cluster velocities have been "zeroed" to -297 km s^{-1}.

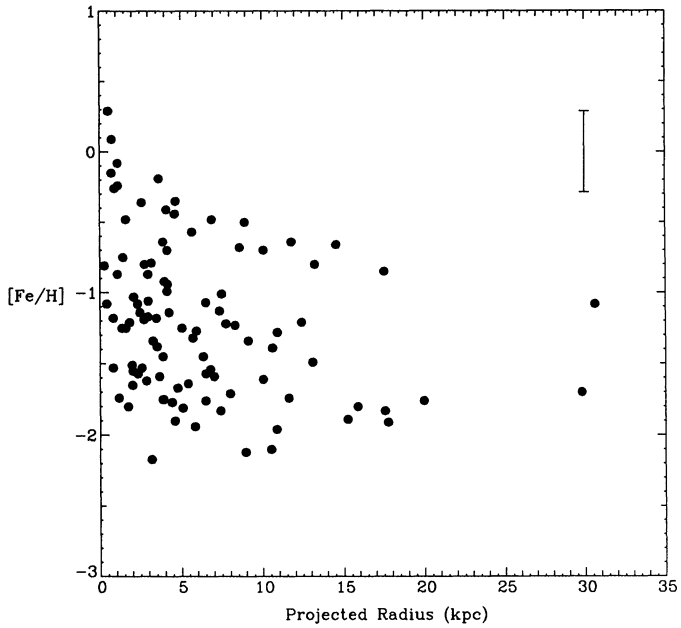

FIG. 2.—Metallicity as a function of projected radius in kpc for the M31 clusters. The distance to M31 is taken to be 690 kpc. Only those (96) clusters for which the metallicity error estimate is less than 0.5 dex are plotted.

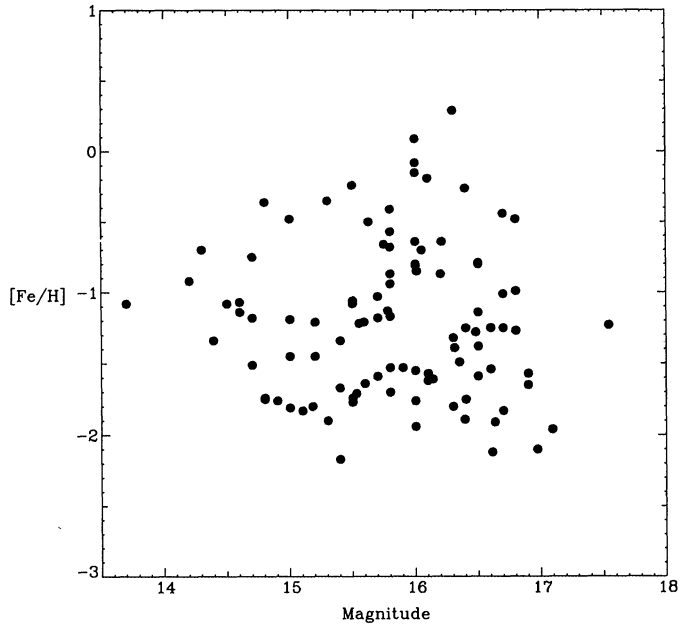

FIG. 3.—Metallicity as a function of apparent magnitude

and decreases with R. Even though the upper envelope of [Fe/H] appears to be decreasing rapidly with radius, the mean decreases much less rapidly. Note that the metallicity is plotted as a function of projected radius. Use of the true radius if it were available, could reduce the scatter and make the gradient more apparent. For comparison, Figure 2 can be compared with Figure 11 from Zinn (1985), which shows metallicity versus radius for the Milky Way "halo" clusters. If the M31 clusters more metal-rich than [Fe/H] $= -0.8$ are excluded from the comparison, the two distributions are very similar. The weighted mean metallicity for all 150 M31 clusters is [Fe/H] $\sim -1.21 \pm 0.02$. This is slightly more metal-rich than the Milky Way's clusters, where the mean [Fe/H] is $\sim -1.40 \pm 0.01$ (the weighted mean derived from the values for the 121 Galactic clusters in Zinn & West 1984). The most metal-rich clusters near M31's nucleus (112-174 and 143-198) appear to have slightly greater than solar abundance.

3.3. [Fe/H] *versus Cluster Luminosity*

The dependence of cluster metallicity on luminosity pertains to various aspects of cluster formation and evolution, i.e., the importance of self-enrichment, the extent to which very massive clusters can retain heavy elements from the first generation of stars, and the ability of protoclusters to sweep up enriched material during passage near the center of the galaxy (van den Bergh 1980). Figure 3 shows the metallicity versus apparent magnitude for the M31 clusters. As is true for the Milky Way's globular clusters (Harris & Racine 1979; van den Bergh 1980), there is no trend of [Fe/H] with luminosity.

Figure 4 shows the metallicity histogram for the same sample as in Figure 2. For comparison we also show the corresponding histogram for Milky Way clusters from Zinn (1985). Allowing for the fact that the metallicity errors for the M31 clusters are significantly larger than those for the Milky Way clusters, the two distributions are consistent with each other. However, there is no obvious bimodality in the M31 distribution, so any division of the clusters into metallicity groups is

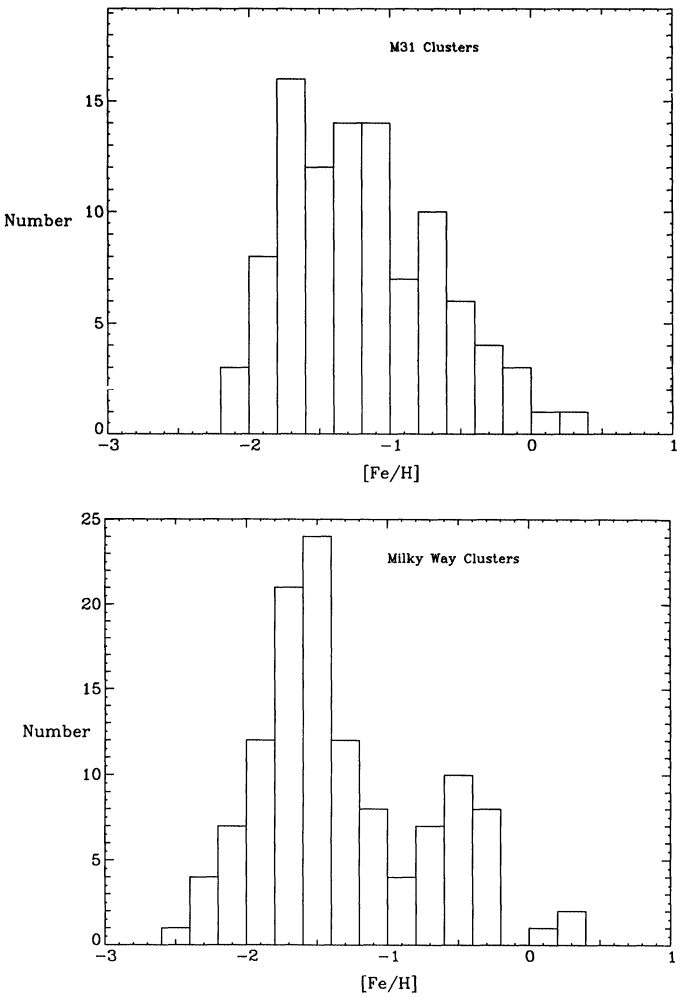

FIG. 4.—Histogram of number vs. metallicity, for the M31 clusters (*top*) and for the Milky Way clusters from Zinn (1985) (*bottom*).

rather arbitrary. On the other hand, bimodality of the cluster distribution might be masked by the size of the errors in the metallicities for the M31 clusters as compared with those for Galactic globulars. For a direct comparison with the Milky Way, we cut the M31 sample at [Fe/H] = −0.8, following Zinn.

Plots of the distribution on the sky of metal-rich and metal-poor clusters (Fig. 5) suggest the metal-rich sample is more centrally concentrated than the metal-poor sample. However, the effect is less pronounced for a magnitude-limited sample. For $m_V \leq 16.5$ mag, we find an effective radius of 3.1 kpc for the metal-rich sample and 3.9 kpc for the metal-poor sample. The result is very similar if the cut is made at [Fe/H] = −1, but if it is made at other values (−0.6, −1.2), the differences between the two groups are marginally less apparent.

3.4. *Rotation of the Cluster System*

The strongest dependence of cluster rotation properties on metallicity is found in the inner 1.5 kpc. Figures 6*a* and 6*b* show that, in this inner region, the metal-rich clusters, again [Fe/H] ≥ −0.8, exhibit a more rapid (100–200 km s^{-1}) rotation than the cluster system as a whole (∼45 km s^{-1}), while the metal-poor clusters are apparently not rotating at all. At larger radii, the cluster system rotation is not so easily separable as a function of metallicity. Table 3 shows how the mean rotational velocities of all clusters, and the metal-rich and the metal-poor clusters separately, depend on radius (at 690 kpc, 1′ is ∼200 pc). The rotation of the metal-rich clusters is slightly weaker, although still present, at larger radii (Fig. 6*c*). It is only slightly more pronounced than the rotation of the metal-poor clusters over the same region (Fig. 6*d*). Beyond 7′, both the metal-rich and the metal-poor clusters appear to be rotating with a semi-amplitude of ∼60 km s^{-1} (or a peak-to-peak amplitude of ∼120 km s^{-1}). The mean velocity for the 48 clusters with $X \geq 10'$ is −227 ± 20 km s^{-1}, and for the 42 clusters with $X \leq -10'$ it is 347 ± 19 km s^{-1}, giving a rotational semi-amplitude of 60 ± 14 km s^{-1}, in very good agreement with the rotational velocity of 80 ± 20 km s^{-1} quoted by HSS. A gradual transition from the metal-rich inner disk population to the metal-poor halo population is implied; there appear to be no sharp boundaries between these population groups.

An additional five clusters have velocities measured by Federici et al. (1990). All of these clusters lie beyond 10′, and so increase the total number of large radius clusters from 90 to 95. When these velocities are added to the sample, the cluster system rotation at large X increases to 62 ± 14 km s^{-1}, and the cluster system as a whole to 46 km s^{-1}.

4. CONCLUSIONS

The M31 cluster system is remarkably similar to the Milky Way system. There is a wide range in metallicity (a factor of 100) that is comparable to that found for Milky Way clusters. As expected on the basis of observations of Milky Way clusters, there is no dependence of metallicity on cluster luminosity for the M31 clusters. The average metallicity, [Fe/H], for the Andromeda clusters is slightly higher than that of the Milky Way's clusters (by about 0.2 dex). The most metal-rich clusters have approximately solar abundance, but earlier indications that the M31 system might be significantly more metal-rich than the Milky Way system are not borne out by our larger sample.

There seems to exist an empirical correlation between a galaxy's luminosity or mass and the mean metallicity of its globular clusters. The existence of such a relationship was first suggested by van den Bergh (1975). Mould, Oke, & de Zeeuw (1990) have shown that mean cluster metallicity and galaxy luminosity are approximately linear related for three dwarf ellipticals and two luminous ellipticals, M49 and M87. In a separate paper we present evidence that a similar relationship

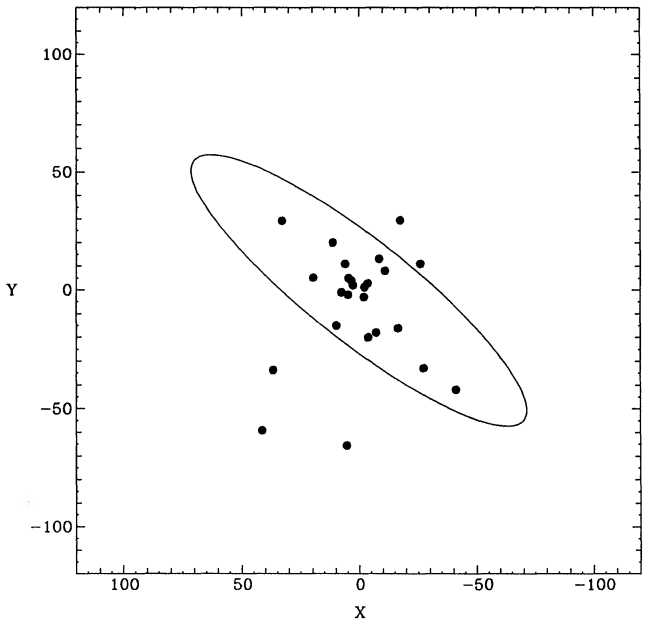

FIG. 5*a*

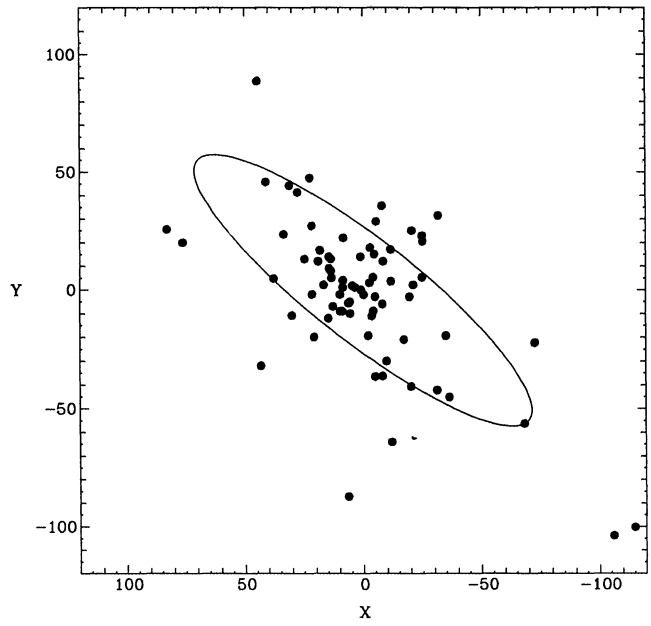

FIG. 5*b*

FIG. 5.—Distribution of clusters on the sky. The ellipse corresponds to the de Vaucouleurs radius. (*a*) Distribution of clusters with [Fe/H] ≥ −0.8; 38 objects. (*b*) Distribution of clusters with [Fe/H] < −0.8; 106 objects.

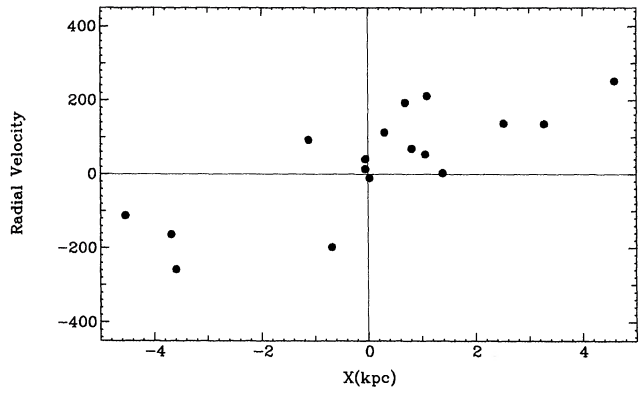

FIG. 6a

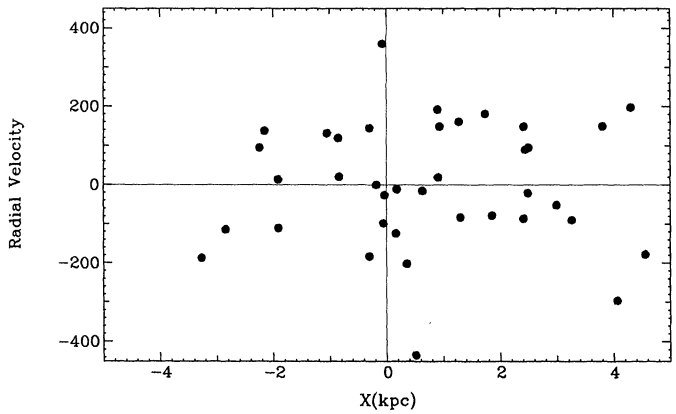

FIG. 6b

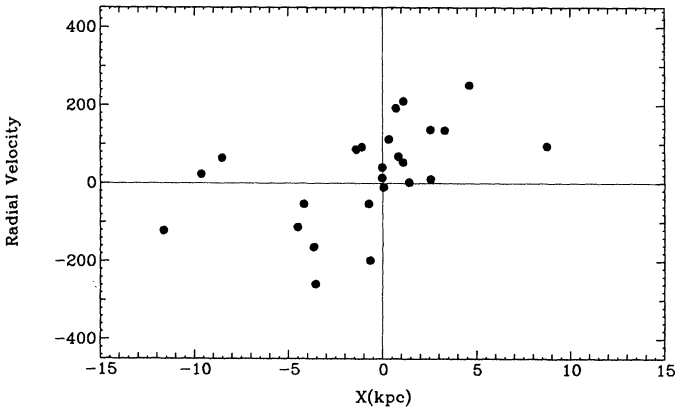

FIG. 6c

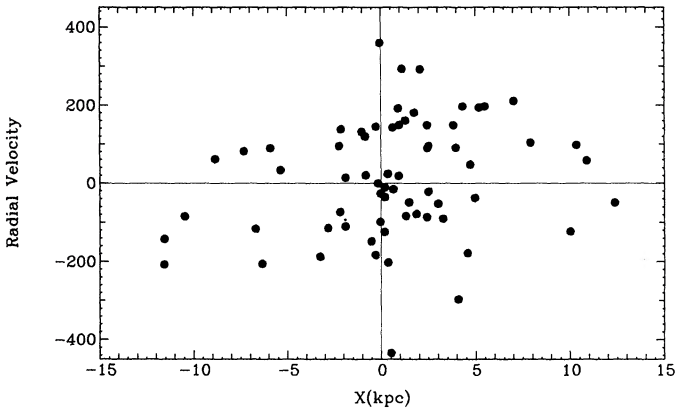

FIG. 6d

FIG. 6.—Radial velocity as a function of projected radius. (*a*) Clusters with [Fe/H] ≥ -0.8 in the inner 5 kpc. (*b*) Clusters with [Fe/H] < -0.8 in the inner 5 kpc. (*c*) Clusters with [Fe/H] ≥ -0.8 out to 15 kpc. (*d*) Clusters with [Fe/H] < -0.8 out to 15 kpc.

TABLE 3

CLUSTER SYSTEM ROTATION

Projected X	0'	1'	2'	3'	4'	5'	7'	10'	15'	25'
All Clusters										
$X \geq 0$	-226	-222	-220	-216	-216	-222	-230	-227	-235	-233
n	(81)	(78)	(71)	(69)	(64)	(59)	(53)	(48)	(37)	(21)
$X < 0$	-316	-322	-322	-320	-317	-322	-337	-347	-357	-342
n	(69)	(62)	(60)	(59)	(56)	(52)	(46)	(42)	(33)	(23)
High Metallicity Clusters ([Fe/H] $\geq$ -0.8)										
$X \geq 0$	-200	-192	-192	-205	-215	-213	-222	-214	-195	-339
n	(19)	(17)	(16)	(15)	(13)	(12)	(10)	(9)	(6)	(3)
$X < 0$	-353	-364	-364	-364	-357	-345	-345	-362	-374	-338
n	(21)	(18)	(18)	(18)	(16)	(15)	(12)	(11)	(10)	(5)
Low Metallicity Clusters ([Fe/H] < -0.8)										
$X \geq 0$	-233	-230	-228	-219	-216	-224	-231	-230	-243	-216
n	(62)	(61)	(55)	(54)	(51)	(47)	(43)	(39)	(31)	(18)
$X < 0$	-299	-304	-304	-300	-301	-312	-334	-342	-350	-343
n	(48)	(44)	(42)	(41)	(40)	(37)	(34)	(31)	(23)	(18)
Rotational Velocity	V_r	km s^{-1}	$(V_{X\geq 0} - V_{X<0})$							
All Clusters	45	50	51	52	51	50	54	60	61	54
High [Fe/H]	77	86	86	80	71	66	62	74		
Low [Fe/H]	33	37	38	41	42	44	51	56	54	64

NOTE.—Numbers refer to the mean heliocentric velocity of the clusters as a function of projected distance from the minor axis. The velocities given are the average of all clusters with projected minor-axis distances *greater than* or *less than* the *X* in the first row. The numbers in parentheses are the integral numbers of clusters in each range.

between [Fe/H] and parent galaxy luminosity holds for several other cluster systems (Brodie & Huchra 1991).

As in the Milky Way, it appears that there is a correlation of cluster [Fe/H] with radius for the M31 clusters. Whether this is best described as a gradient, a decrease in the upper "envelope" of abundance, or just a statistical (population) effect is difficult to say without more data and a more detailed analysis.

The high-metallicity clusters in M31 appear to form a central rotating disk system, although the distinction between halo and disk is not as marked as in the Milky Way, perhaps because of projection effects. Projection effects, however, cannot account for the similarity in rotation of M31's metal-rich and metal-poor clusters at large radii. At projected radii greater than 10′, the M31 cluster system is rotating with a velocity of ~ 60 km s^{-1}, again similar to the rotation velocity of the Milky Way cluster system.

The mass of M31 derived from the velocity observations is consistent with mass estimates from other techniques. The blue mass-to-light ratio is typical of massive spirals, ~ 40 in solar units [in the uncorrected $B(0)$ system; Huchra 1976], or ~ 16 in the B_T^0 system. This M/L is both well above the M/L predicted from simple stellar population models of the galaxy's bulge + disk and also well below the "critical" M/L which would be required if the mass in galaxies were to close the universe (about 2400 in solar units for a Hubble constant of 100 km s^{-1}). As usual, if the M/L of M31 is typical, Ω_G, the ratio of the observed mass density in galaxies to the closure mass density, is only a few percent.

We would like to thank Susan Tokarz and Cathy Clemens for help with the data reduction and table entry. We would like to thank Bill Baum, Dave Burstein, Judy Cohen, Sandy Faber, Flavio Fusi Pecci, Leonard Searle, and Sidney van den Bergh for helpful discussions and for communicating data in advance of publication. We would also like to thank the anonymous referee for useful corrections. This work has been supported by the Smithsonian Institution, by faculty research funds from the University of California, Santa Cruz, and by NSF grant AST-8451724.

REFERENCES

Baade, W., & Arp, H. 1964, ApJ, 139, 1027
Bahcall, J., & Tremaine, S. 1981, ApJ, 244, 805
Battistini, P., Bónoli, F., Braccesi, A., Federici, L., Fusi Pecci, F., Marano, B., & Borngen, F. 1987, A&AS, 67, 447
Battistini, P., Bónoli, F., Braccesi, A., Fusi Pecci, F., Malagnini, M., & Marano, B. 1980, A&AS, 42, 357
Bónoli, F., Federici, L., & Fusi Pecci, F. 1988, A&A, 205, 6
Brodie, J., & Huchra, J. 1990, ApJ, 362, 503
———. 1991, ApJ, in press
Buonano, R., Corsi, C., Battistini, P., Bónoli, F. & Fusi Pecci, F. 1982, A&AS, 47, 451
Cohen, J. 1987, private communication
Crampton, D., Cowley, A. P., Schade, D., & Chayer, P. 1985, ApJ, 288, 494
Cromwell, R., & Weymann, R. 1982, private communication.
Elson, R., & Walterbos, R. 1988, ApJ, 333, 594
Faber, S., & Gallagher, J. 1979, ARA&A, 17, 135
Federici, L., Fusi Pecci, F., & Marano, B. 1990, A&A, in press
Freeman, K. 1983, in IAU Symposium 100, Internal Kinematics and Dynamics of Galaxies, ed. E. Athanassoula (Dordrecht: Reidel), 359
———. 1985, in IAU Symposium 106, The Milky Way Galaxy, ed. H. van Woerden (Dordrecht: Reidel)
Frenk, C., & White, S. 1980, MNRAS, 193, 295
———. 1982, MNRAS, 198, 173
Harris, W. E., & Racine, R. 1979, ARA&A, 1, 241
Heisler, J., Tremaine, S., & Bahcall, J. 1985, ApJ, 298, 8
Hubble, E. 1932, ApJ, 76, 44
Huchra, J. 1976, AJ, 81, 952
Huchra, J., & Brodie, J. 1984, ApJ, 280, 547
———. 1987, AJ, 93, 779
Huchra, J., Brodie, J., Stauffer, J., & Caldwell, N. 1991, ApJS, in preparation
Huchra, J., Stauffer, J., & van Speybroeck, L. 1982, ApJ, 259, L57 (HSS)
Kent, S. 1989, AJ, 97, 1614
Kent, S., Huchra, J., & Stauffer, J. 1989, AJ, 98, 2080
Kron, G. E., & Mayall, N. U. 1960, AJ, 65, 581
Latham, D. 1982, in Instrumentation for Astronomy with Large Optical Telescopes, ed. C. M. Humphries (Dordrecht: Reidel), 259
Mayall, N. U., & Eggen, O. J. 1953, PASP, 65, 24
Mould, J. R., Oke, J. B., & de Zeeuw, P. T. 1990, AJ, in press
Peterson, R. 1990, in Dynamics of Dense Stellar Systems, ed. D. Merrit (Cambridge: Cambridge Univ. Press)
Roberts, M. S., & Whitehurst, R. N. 1975, ApJ, 201, 327
Rubin, V. C., & Ford, W. K. 1970, ApJ, 159, 379
Sargent, W. L. W., Kowal, C., Hartwick, F. D. A., & van den Bergh, S. 1977, AJ, 82, 947
Searle, L. 1983, private communication
Seyfert, C., & Nassau, J. 1945, ApJ, 102, 377
Spinard, H., & Schweizer, F. 1972, ApJ, 171, 403
Tonry, J., & Davis, M. 1979, AJ, 84, 1511
van den Bergh, S. 1969, ApJS, 19, 145
———. 1975, ARA&A, 13, 217
———. 1980, in Globular Clusters, ed. D. Hanes & B. Madore (Cambridge: Cambridge Univ. Press), 175
———. 1981, PASP, 93, 428
Vetesnik, M. 1962, Bull. Astr. Inst. Czechoslovakia, 13, 180
Zinn, R. 1985, ApJ, 293, 424
———. 1986, in Stellar Populations, ed. C. Norman, A. Renzini, & M. Tosi (Cambridge: Cambridge Univ. Press), 73
Zinn, R., & West, M. 1984, ApJS, 55, 45